Absorption and fluorescence of chromophoric dissolved organic matter in the Pearl River Estuary, South China

Huasheng Hong [a], Jingyu Wu [a], Shaoling Shang [a,*], Chuanmin Hu [b]

[a] *State Key Laboratory of Marine Environmental Science (Xiamen University), Xiamen University, Xiamen, Fujian 361005, China*
[b] *College of Marine Science, University of South Florida, 140 7th Avenue South, St. Petersburg, FL 33701, USA*

Abstract

The Pearl River is a complex river network under the influence of heavy urbanization and industrialization. The Pearl River Estuary receives freshwater from eight major sources, each containing various pollutants. The spectral absorption and fluorescence properties of chromophoric dissolved organic matter (CDOM) in the Pearl River Estuary were studied during November 2002, a low flow (dry) season. Over a salinity range of 33–0, CDOM absorption coefficients at 355 nm (a(355)) ranged from 0.24 to 1.93 m^{-1}, lower than several other American and European estuaries. In contrast to the wet season, conservative mixing was evidenced by a linear, inverse relationship between a(355) and salinity. CDOM, primarily of terrestrial origin, contained more anthropogenic organic matter than natural plant decay matter: tryptophan-like fluorophore T had the strongest signal among all fluorophores for the entire study region. The absorption spectral slope (S), determined between 300 and 500 nm, ranged between 0.0138 and 0.0184 nm^{-1} and did not show distinguishable patterns except in the transition zone between the estuary and the South China Sea. The relative composition of fluorophores was found to vary among different sources. This result demonstrated the potential for using fluorophores to characterize the composition of CDOM and trace pollutants to their various freshwater sources.
© 2005 Elsevier B.V. All rights reserved.

1. Introduction

Chromophoric dissolved organic matter (CDOM), an optically active component of dissolved organic matter, mainly originates from degradation of plant materials in terrestrial and aquatic ecosystems (Kirk, 1994). It plays an important role in carbon cycling and affects ocean color. CDOM in estuaries and coastal regions is typically of terrestrial origin (i.e., land drainage and/or river discharge (Blough and Del Vecchio, 2002)). Knowledge of CDOM distributions and spectral characteristics is important for identifying CDOM sources, compositions, and fates. Further,

---

* Corresponding author. Tel.: +86 592 2184781; fax: +86 592 2188071.
E-mail addresses: slshang@jingxian.xmu.edu.cn, slshang@gmail.com (S. Shang).

because CDOM is typically a conservative variable, it can be used to assess the physical mixing of other water constituents such as trace metals and pollutants. This is particularly useful since CDOM can in principle be determined with remote sensing techniques. In offshore waters, CDOM is presumably related to phytoplankton degradation and/or zooplankton grazing (Siegel and Michaels, 1996; Momzikoff et al., 1994; Carder et al., 1989; Yentsch and Reichert, 1961; Fogg and Boalch, 1958). Although the global and regional surface distribution of CDOM can be remotely estimated with moderate accuracy (e.g., Siegel et al., 2002; Hu et al., 2003), in estuaries and coastal waters such exercises are often hindered by the optical complexity of these environments. In particular, spectroscopic information on CDOM in major world river systems is rarely available, except for a few studies that lack continuity in both space and time (e.g., Blough et al., 1993; Del Castillo et al., 2001).

Ranked 13th in the world by discharge volume, the Pearl River is the largest river in South China (Fig. 1) (Huang et al., 2003). Its mean annual discharge volume is about 336,000 million m^3. The period of high flow, from April to September, accounts for 80%

of the annual discharge volume. Low flow season is from October to March, and the flushing time is about 22 days during this season (Chen et al., 1993). The Pearl River system is a complex network of numerous river tributaries and channels. Freshwater containing dissolved and particulate materials, both anthropogenic and natural, flows out of eight river outlets, through the Pearl River Estuary into the South China Sea (Pearl River Water Resources Commission, Ministry of Water Resources, China, http://www.pearlwater.gov.cn). The estuary is surrounded by several big cities including Guangzhou, Shenzhen, Hong Kong, and Macau. Following China's economic reforms since 1978, the entire Pearl River Delta Region has been one of the most quickly developing regions in China and Asia. Therefore, impacts of heavy urbanization and industrialization on the estuary waters have been inevitable. As one example, the frequency of red tide events appears to be increasing. Since the 1970s, more than one hundred red tide events have been reported in this region (Qian and Liang, 1999).

Because riverine and marine CDOM end members often mix conservatively (Nieke et al., 1997; Vodacek
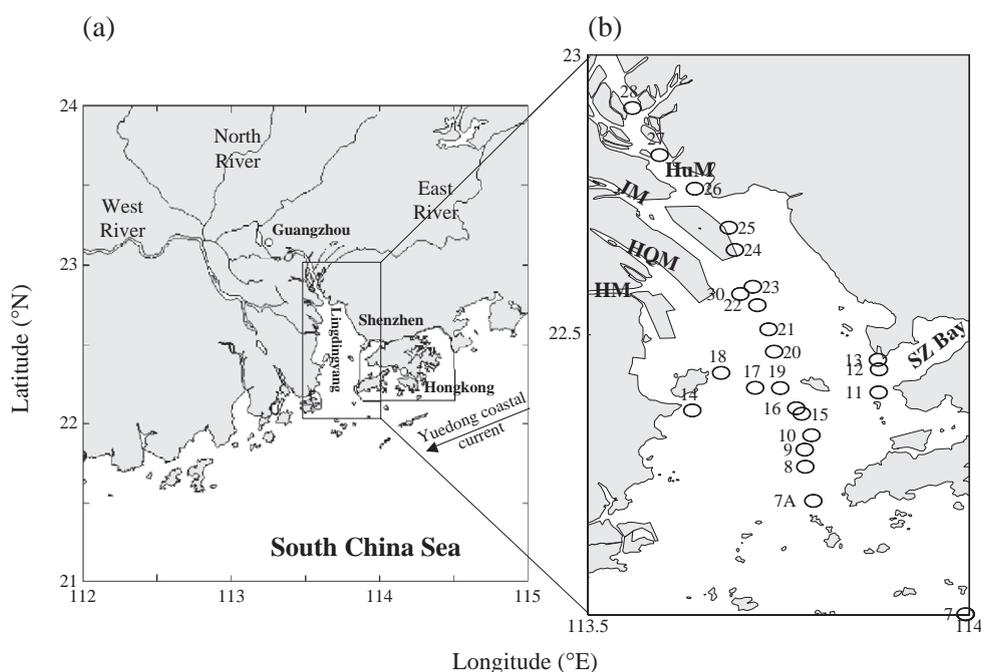

Fig. 1. (a) Location of the Pearl River network and the Pearl River Estuary; (b) Sampling stations in Lingdingyang. Four outlets (Humen, Jiaomen, Hongqimen and Hengmen) and Shenzhen Bay are marked as HuM, JM, HQM, HM, and SZ Bay, respectively.

et al., 1997; Siddorn et al., 2001), and CDOM can potentially be estimated synoptically from space, it is desirable to establish a database that describes CDOM spatial and spectral distributions and their temporal variations. In this regard, in situ sampling, covering an appropriate dynamic range and various CDOM sources, is a necessary first step towards improved utilization of remote sensing for assessment of estuarine water quality and estuarine mixing.

Literature data for CDOM in the Pearl River Estuary are rare. A 1999 summer survey (Chen et al., 2004) found that CDOM concentrations were lower than those from some American and European estuarine waters. The estuary's CDOM absorption coefficients at 355 nm ($a(355)$, a proxy for CDOM concentration) ranged from 0.34 to 1.40 m^{-1}. There was no clear relationship between CDOM and salinity. In a broader region from the Pearl River Estuary to the South China Sea shelf water, Chen et al. (2003) measured the CDOM absorption coefficient in summer 2002. In the estuary itself, $a(400)$ varied from 0.51 m^{-1} (salinity near 30) to 1.42 m^{-1} near the river mouth (salinity near 1). The slope parameter of the CDOM absorption spectrum (S) ranged from 0.013 to 0.018 nm^{-1}. The wavelength range from which S was determined was not reported and the $a(400)$ vs. salinity relationship was non-linear. Callahan et al. (2004) presented results of fluorescent dissolved organic matter (FDOM) measurements obtained in the Pearl River Estuary and the adjacent South China Sea during a study of dissolved organic carbon (DOC) in May 2001 and November 2002. FDOM fluorescence and DOC concentrations were found to be linearly correlated in part of the study region. Since the study focused on DOC, optical properties of CDOM were not reported except for limited fluorescence data (in either Quinine Sulfate Units or arbitrary units).

The two pioneering studies of CDOM in the region (Chen et al., 2003, 2004) had different objectives and used two different reference wavelengths, 355 and 400 nm, respectively. This makes comparisons difficult, as the spectral slope parameter was either not reported, or was reported without the applicable wavelength range. Although the two field surveys were carried out in summer, a high flow season, they did not show a consistent relationship between CDOM and salinity. These surveys were limited in their spatial and temporal coverage and in the number of measured variables. Clearly, CDOM characteristics in the Pearl River Estuary are still poorly known.

This work reports CDOM absorption and fluorescence characteristics of Pearl River Estuary obtained during extensive winter sampling in 2002 (a low flow season). These data were obtained to complement previous studies and to improve our understanding of the estuary's CDOM abundance, spatial and temporal variability, and spectrochemical characteristics. Several specific questions addressed in this paper include:

(1) How does CDOM vary spatially in the low flow season?
(2) What were the causative factors for the observed distributions?
(3) Were there any spectral signatures (e.g., absorption spectral slope, fluorescence excitation and emission maxima) of CDOM samples collected adjacent to freshwater outlets that could lead to identification of CDOM sources?

2. Methods

2.1. Study region

Our study focused on the main part of the Pearl River Estuary, the Lingdingyang. Fig. 1 shows the sampling locations, from Stations 7 to 30. Lingdingyang has four freshwater sources (Humen, Jiaomen, Hongqimen, and Hengmen). These inputs contribute freshwater as well as dissolved and particulate materials to the estuary, whose depth ranges from 5 m to more than 20 m.

2.2. Sample collection

Water samples were collected during a cruise on the R/V Yanping-II from 2 to 21 November 2002. The entire procedure, including sample collection, storing and measurement, was performed strictly according to the Ocean Optics Protocols Version 2.0, distributed by NASA (Mitchell et al., 2000). Briefly, water was collected with 1.7 L Niskin bottles mounted on a rosette along with a SBE19 CTD. Only surface water was sampled at shallow stations. At relatively deep stations, middle layer and near bottom water was

also sampled, depending on the depth of each station. Water samples were filtered with thoroughly cleaned 0.2 μm Millipore polycarbonate filters, and then stored at −26 °C in pre-combusted amber-colored glass bottles for subsequent laboratory analysis at the Xiamen University. The frozen samples were warmed to room temperature in a water bath before analysis.

2.3. Absorption spectroscopy

Absorbance (A) was measured in a 10-cm quartz cell using a Varian Cary-100 dual-beam spectrophotometer. The absorbance precision of this instrument was ±0.003. Absorption coefficients (a) were calculated (Hu et al., 2002) at 1 nm intervals between 250 and 800 nm:

$$a(\lambda) = 2.303 A(\lambda)/r \qquad (1)$$

where λ is wavelength and pathlength (r) is 0.1 m.

To remove residual errors from either scattering or instrument noise, a nonlinear least square regression was employed to obtain the spectral slope (S) over a wavelength range from 300 to 500 nm:

$$a(\lambda) = a(\lambda_0)\exp[-S(\lambda - \lambda_0)] + K \qquad (2)$$

where K is an offset at the wavelength of infinity (i.e., where $a(\lambda_0)\exp[-S(\lambda - \lambda_0)]=0$) and λ_0 is a reference wavelength. The assumption here is that residual scattering and/or noise are spectrally flat. After regression, K was discarded and $a(\lambda)=a(\lambda_0)\exp[-S(\lambda - \lambda_0)]$ was used as the spectral absorption coeffi-

cient (Markager and Vincent, 2000). To facilitate comparison with other studies, a(355) was chosen as an index for CDOM abundance.

2.4. Fluorescence excitation–emission matrix spectra

Fluorescence was measured with a Varian Cary Eclipse fluorescence spectrophotometer. Emission spectra were measured every 2 nm from 260 to 710 nm at 49 excitation wavelengths between 210 and 450 nm (Coble, 1996; Coble et al., 1998). A Milli-Q water blank correction was applied to eliminate water-Raman peaks. As described by Coble et al. (1998), fluorescence intensity was normalized to a quinine sulfate standard and expressed as quinine sulfate equivalent (QSE) in parts per billion (ppb). Results were then combined to generate a plot of Excitation–Emission Matrices (EEMs) with the software Surfer. Due to instrumental limitations, fluorescence data were not corrected for optical aberrations (various instrument-dependent characteristics of grating, lamp, mirror, etc.).

3. Results and discussion

3.1. Abundance of CDOM

a(355) ranged from 0.24 m^{-1} at salinity 32.9, to 1.93 m^{-1} at salinity near zero. Absorption coefficients were relatively low compared to other estuaries and coastal waters (Table 1). As shown by AVHRR NDVI

Table 1
Absorption coefficients (m^{-1}) and spectral slopes ($\times 10^3$ nm^{-1}) of CDOM from some estuarine and coastal waters in the world, as well as from this study

| Region	Salinity range	a(355)	S ($\times 10^3$ nm^{-1})	Reference
Amazon River Estuary	15.1–36.4	0.14–3.12	15–33	Green and Blough (1994)
Tamiami River	–	33.7	17	Green and Blough (1994)
Orinoco River	–	22.6–57.3 (a(300))	8.6–13.9	Battin (1998)
Surumoni River	–	14.7–151.1 (a(300))	8.5–15.2	Battin (1998)
Eastern Carribean Sea (near Orinoco River)	19.7–33.7	0.3–9.1 (a(300))	12–20	Del Castillo et al. (1999)
Chesapeake Bay				Rochelle-Newall and Fisher (2002)
April	~13–33	0.5–2.2	–	
October	~5.8–27	0.7–2.1	–	
Southern Baltic Sea (coastal areas)	–	1.4–12.8	–	Ferrari and Dowell (1998)
Gulf of Lions (near Rhone River mouth)	34–38.2	0.05–1.71	11–27	Ferrari (2000)
Pearl River Estuary (July)	0–34.96	0.34–1.40	–	Chen et al. (2004)
Pearl River Estuary (November)	0–32.49	0.24–1.93	13.8–18.4	This study
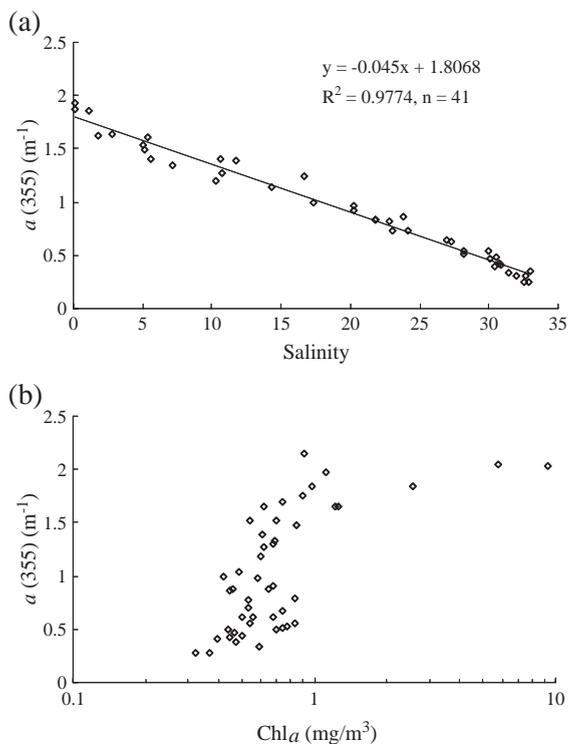
Fig. 2. Absorption coefficients of CDOM at 355 nm ($a(355)$) versus salinity (a) and Chl$a$ (b) for the 41 samples collected from the 24 stations.

servative mixing of freshwater and seawater endmembers. The contribution of local phytoplankton degradation to CDOM appeared to be minor.

Our results contrast with those of Chen et al. (2003, 2004), which showed non-linearity between CDOM and salinity during the wet season (summer). This suggests that the mechanisms controlling the CDOM input to the estuary are possibly more complex in summer than in winter. For example, there might be enhanced phytoplankton degradation during summer as Chl$a$ is typically high (Bangqin Huang et al., Xiamen University, unpublished data). Also, non-point sources of CDOM along the entire estuary, induced by relatively heavy rainfall in summer, might be another controlling factor.

The variations of $a(355)$, salinity, and Chl$a$ in the surface water along the transect from the outer estuary to the inner estuary are shown in Fig. 3. Generally,
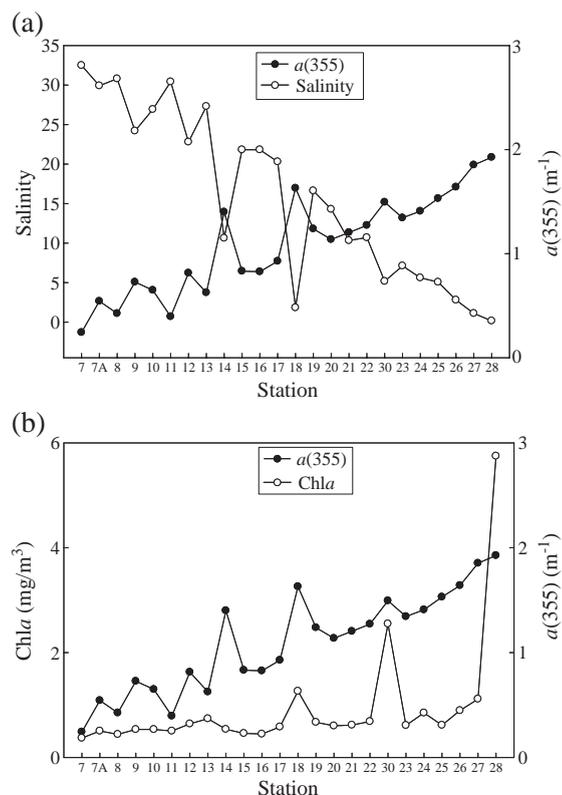
images, this was possibly due to the low degree of vegetative cover in the Pearl River drainage basin. Comparison with Chen et al. (2004) showed that over the 0–10 salinity range, $a(355)$ from the 2002 dry season was higher than that during a wet season (July 1999), suggesting either interannual variability or evaporation effects. Rainfall in the Southern China coastal region in 1999 was 10% less than the long-term climatological mean (Pearl River Water Resources Commission, Ministry of Water Resources, China, 2000). The resulting low river flow may have led to a relatively low CDOM abundance in the 1999 wet season.

3.2. Distribution and source of CDOM

The linear relationship between $a(355)$ and salinity (Fig. 2) indicated that freshwater was the primary source of CDOM in the Pearl River Estuary, and that CDOM concentrations were controlled by con-

Fig. 3. Horizontal distribution of absorption coefficients of CDOM at 355nm ($a(355)$) and salinity (a), Chl$a$ (b) in the surface water from the outer estuary to the inner estuary. Note that Station 30 was located between Stations 22 and 23 (see Fig. 1).
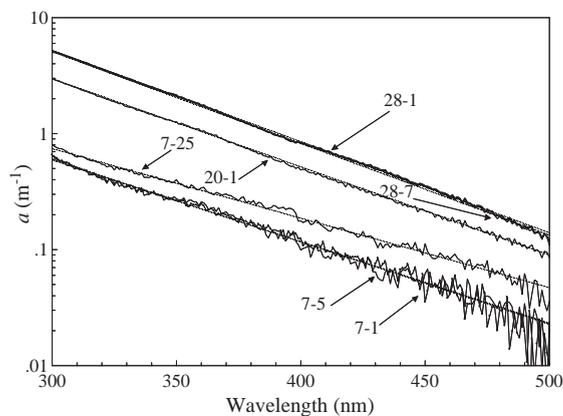
Fig. 4. Absorption spectra of CDOM at three stations, representing the riverine water (Station 28), the intermediate water (Station 20), and the marine water (Station 7), respectively. Solid and dotted lines indicate measured and fitted spectra, respectively. Annotations indicate sampling station and depth, e.g., 7–25 means Station 7 at 25 m depth.

$a(355)$ increased toward the inner estuary. Peaks in $a(355)$ and/or Chl$a$ were found at Stations 14, 18, 30, and 28, which were located in the vicinity of several freshwater outlets. Stations 14 and 18 were near Hengmen and Hongqimen, and Station 30 was close to Jiaomen. Station 28, upstream of Humen, showed the highest Chl$a$, lowest salinity, and the highest $a(355)$ in the surface water. The variation of $a(355)$ with geographical locations demonstrated the existence of independent terrestrial CDOM inputs at each freshwater outlet. However similar end member CDOM abundances in the various outlets are suggested by the linear relationship between $a(355)$ and salinity. Clearly, the $a(355)$-salinity relationship can not be used to trace the origin of a particular sample.

Chl$a$ showed much smaller variations than $a(355)$ along the transect (Fig. 3b). Most stations showed Chl$a \leqq 1$ mg/m^3, corresponding to an absorption coefficient of $\leqq 0.04$ m^{-1} at 440 nm for Chl$a$, while the $a(440)$ of CDOM was five to ten times higher ($\leqq 0.41$ m^{-1}). These results suggested (1) that the estuary was a typical Case-II water (Morel and Prieur, 1977) where Chl$a$ was neither the dominant component affecting optical properties nor co-varied with CDOM, and (2) that color variability, as viewed from space, was principally due to CDOM and suspended particle matter rather than Chl$a$. Distinguishing Chl$a$ from CDOM by means of remote sensors for

this type of complex environment therefore presents a great challenge to the community.

3.3. CDOM spectral characteristics

3.3.1. Absorption spectral slopes

Fig. 4, showing typical CDOM absorption spectra from Stations 28, 20, and 7, demonstrates how spectral slope changed between riverine water, intermediate water, and marine water. There was a measurable difference in the slope between Station 7 and the other two stations, especially at the 25-m depth of Station 7.

The spectral slope parameter, S, determined over a spectral range from 300 to 500 nm, was studied to see if any spatial distribution patterns might be observed. Fig. 5a shows S vs. salinity for all stations. S varied between 0.0138 and 0.0184 nm^{-1}, consistent with observations from other coastal waters that received
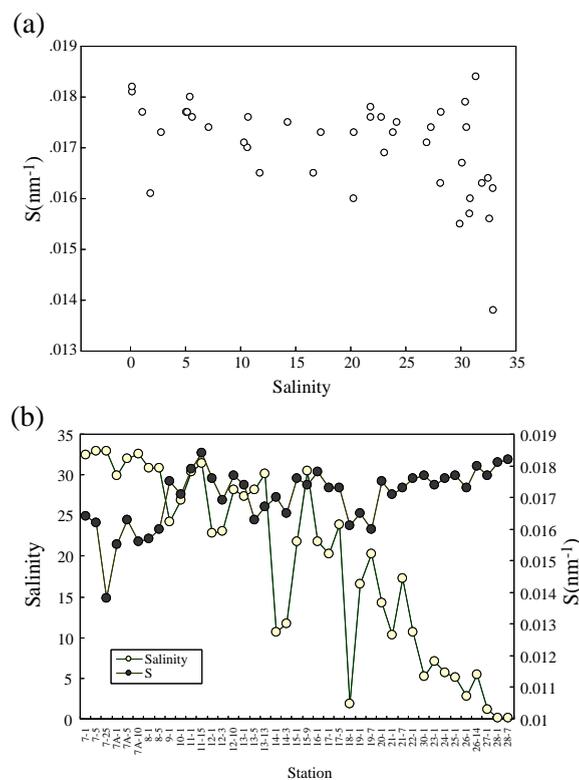

Fig. 5. (a) Salinity versus CDOM absorption spectral slope (S), obtained over a spectral range of 300 to 500 nm for all samples; (b) Variation of S and salinity from the outer estuary to the inner estuary. The X-axis labels indicate each sampling station and depth, e.g., 7–5 means Station 7 at 5 m depth.

river inputs (e.g., Carder et al., 1989; Blough et al., 1993). Excluding the minimum at high salinity, S fluctuated within a range of 0.003 nm^{-1} for all sampling stations (Fig. 5a).

Although there was no apparent pattern for most stations, S tended to decrease near the transition zone that connected the estuary to the shelf water (Stations 8, 7A and 7). Although S usually increases with decreasing absorption and increasing salinity in transition zones (e.g., Blough et al., 1993), cases with low S in high salinity waters similar to that shown in Fig. 5 have also been reported (e.g., Stedmon et al., 2000).

There are several potential sources of CDOM in the transition zone: upstream estuarine water, Hong Kong coastal water, Yuedong Coastal Current and South China Sea shelf water, and CDOM produced in situ from phytoplankton degradation. During winter, the prevailing northeast monsoon drives the Yuedong Coastal Current southwestward along the Guangdong coast. Coastal waters near Hong Kong, rich in anthropogenic organic materials, might have partially influenced the CDOM in the transition zone as a result of hydrodynamic forcing. The marine CDOM input appeared to be multi-source as well, although this influence was weak due to the low concentrations suggested by the $a(355)\sim$ salinity relationship (see Section 3.2). However, S values of marine end members, before entering the transition zone, were unknown. The terrestrial CDOM from upstream estuarine water had relatively high S values and, as noted (Section 3.2), contribution of phytoplankton degradation to the CDOM pool was minor.

Both terrestrial and marine CDOM can be altered by photodegradation and bacterial utilization, leading to changes in S values (Gao and Zepp, 1998; Moran et al., 2000). Currently there is no consensus about these effects on S values, possibly due to different CDOM compositions in different waters.

Considering these complexities, without knowledge of the chemical composition of the CDOM and the bacterial community in the Pearl River Estuary and its adjacent waters, it is difficult to identify the dominant factor resulting in low S values in the transition zone. Because S did not show any apparent patterns for most stations, it cannot be used as an indicator of CDOM source for most of the estuary. Note that the absolute value of S can change slightly with different choice of wavelength range. Hence, comparison of the absolute magnitudes of S among studies should be viewed with caution.

3.3.2. EEM spectroscopy

Fluorescence intensities (F, in parts per billion (ppb) of quinine sulfate equivalent) and excitation–emission (EX/EM) maxima for fluorophores are presented in Table 2. Here we referred to Mopper and Schultz (1993), Coble (1996), Coble et al. (1998), and Blough and Del Vecchio (2002) to classify and label fluorophores. Three distinct principal fluorophore types were observed: tryptophan-like (T), UV humic-like (A) and visible-terrestrial humic-like (C) fluorophores. Fig. 6a shows the EEMs for the Station 28 surface sample, which is representative of the fluorescence features found in most of the study region. In one instance, a marine fluorophore (visible-marine humic fluorophore (M)) was observed for 5 and 25 m depths at Station 7 (Fig. 6b). This provided additional evidence of marine CDOM in the transition zone.

Tryptophan-like fluorophores provided the strongest signals among all fluorophores for all samples. This contrasts with results from other estuarine waters. In the Orinoco river plume, A, C, and M were very strong, while T was only found at 75 m at one station. The occurrence of T was attributed to bacterial degradation of sinking particulate organic matter (Del Castillo et al., 1999). The dominant T signal in the Pearl River Estuary, which had low biomass, suggested that the CDOM might result primarily from sewage, with fluorescence properties similar to animal farm wastes (Baker, 2002). Terrestrial humic or fulvic substances were minor. This is not a surprising result, as the Pearl River drainage basin is heavily industrialized and urbanized. Forest and cropland are scarce, leading to relatively less CDOM produced from decayed plant matter leaching from soils into the river. On the other hand, more than 70% of the pollutants produced in the entire Guangdong province are transported through the Pearl River network into the estuary (Pang and Li, 2001).

There were no significant changes in the EX/EM maxima until the estuarine water reached the transition zone, and most of the EX/EM maxima were similar to those at Station 28 (Fig. 6a; Table 2). For

Table 2
Fluorescence intensities (F) and excitation–emission maxima (EX/EM$_{max}$) in nanometers for fluorophores T, A, C and M

Sample ID	EX/EM$_{max}$ of T	F of T	EX/EM$_{max}$ of A	F of A	EX/EM$_{max}$ of C/M	F of C/M
7-1	–	–	–	–	–	–
7-5	230/352	3.7	–		300/376	3.18
7-25	230/344	3.00	–			
7A-1	230/342	7.44	250/470	3.22		
7A-5	230/342	1.85	–	–	–	–
7A-10	230/338	1.79	–	–	–	–
8-1	230/346	5.33	245/442	2.83		
8-5	230/338	6.62	245/414	4.49		
9-1	230/344	15.28	250/446	7.80	330/434	5.15
10-1	230/344	15.78	250/460	7.50	325/410	4.38
11-1	230/342	9.47	250/454	3.99	325/414	2.51
11-15	230/342	9.42	250/444	3.40	320/404	2.57
12-1	230/346	20.65	250/454	11.19	325/402	5.35
12-3	230/342	19.65	250/462	9.77	325/412	4.79
12-10	230/352	13.88	250/458	5.96	320/422	2.80
13-1	230/344	16.93	250/452	7.55	325/408	3.66
13-5	230/346	11.56	250/454	4.57	315/416	2.51
13-13	230/344	11.10	250/434	4.75	320/404	2.51
14-1	230/342	24.36	250/448	15.35	325/408	8.28
14-3	230/352	21.87	250/456	14.82	325/410	7.47
15-1	230/346	21.08	250/452	11.84	320/408	7.37
15-9	230/352	12.11	245/446	6.73	325/402	4.72
16-1	230/342	22.14	250/454	13.08	315/410	8.49
17-1	230/342	23.81	250/450	14.16	320/422	8.78
17-5	230/344	22.08	250/448	13.63	330/428	8.11
18-1	230/358	27.18	250/448	22.27	325/414	14.58
19-1	230/346	24.57	250/456	15.54	320/422	7.68
19-17	230/346	22.34	250/456	13.08	320/408	7.12
20-1	230/344	28.52	250/452	18.62	320/404	9.00
21-1	230/344	30.98	250/462	21.37	325/422	11.12
21-7	230/344	25.60	250/446	14.33	330/416	8.15
22-1	230/342	31.82	250/454	20.99	330/426	10.78
23-1	230/344	32.44	250/448	21.08	320/410	10.65
24-1	230/344	36.10	250/450	24.51	330/426	12.32
25-1	230/346	39.07	250/456	28.41	325/436	13.25
26-1	230/344	46.64	250/456	32.39	330/416	15.40
26-14	230/348	41.77	250/454	30.09	325/406	13.75
27-1	230/352	53.46	250/456	38.45	330/426	16.75
28-1	230/348	68.76	250/450	35.21	330/416	18.54
28-7	230/348	69.20	250/454	36.97	320/422	19.82
30-1	230/346	35.27	250/450	24.32	315/414	11.6

Fluorescence intensities are expressed as parts per billion (ppb) of quinine sulfate equivalent.

Sample ID indicates each sampling station and depth, e.g., 7-1 means station 7 at 1 m depth; C/M denotes fluorophore C or M.

example, the EX/EM maxima of Station 20 at 1 m depth also showed T, A, and C components (Fig. 6c), although with low intensity. Decrease in fluorescence intensity possibly resulted from dilution (i.e., mixing between estuarine water and seawater). These results are consistent with the observed conservative behavior of CDOM during this season (Section 3.2).

Study of CDOM compositional differences between different outlets was first attempted by comparing the proportions of the three main fluorophores defined as the fluorescence intensity ratio T/A/C. Because the EX/EM maxima changed slightly among samples (Table 2), we adopted consistent EX/EM maxima for all samples (230/346, 250/454,
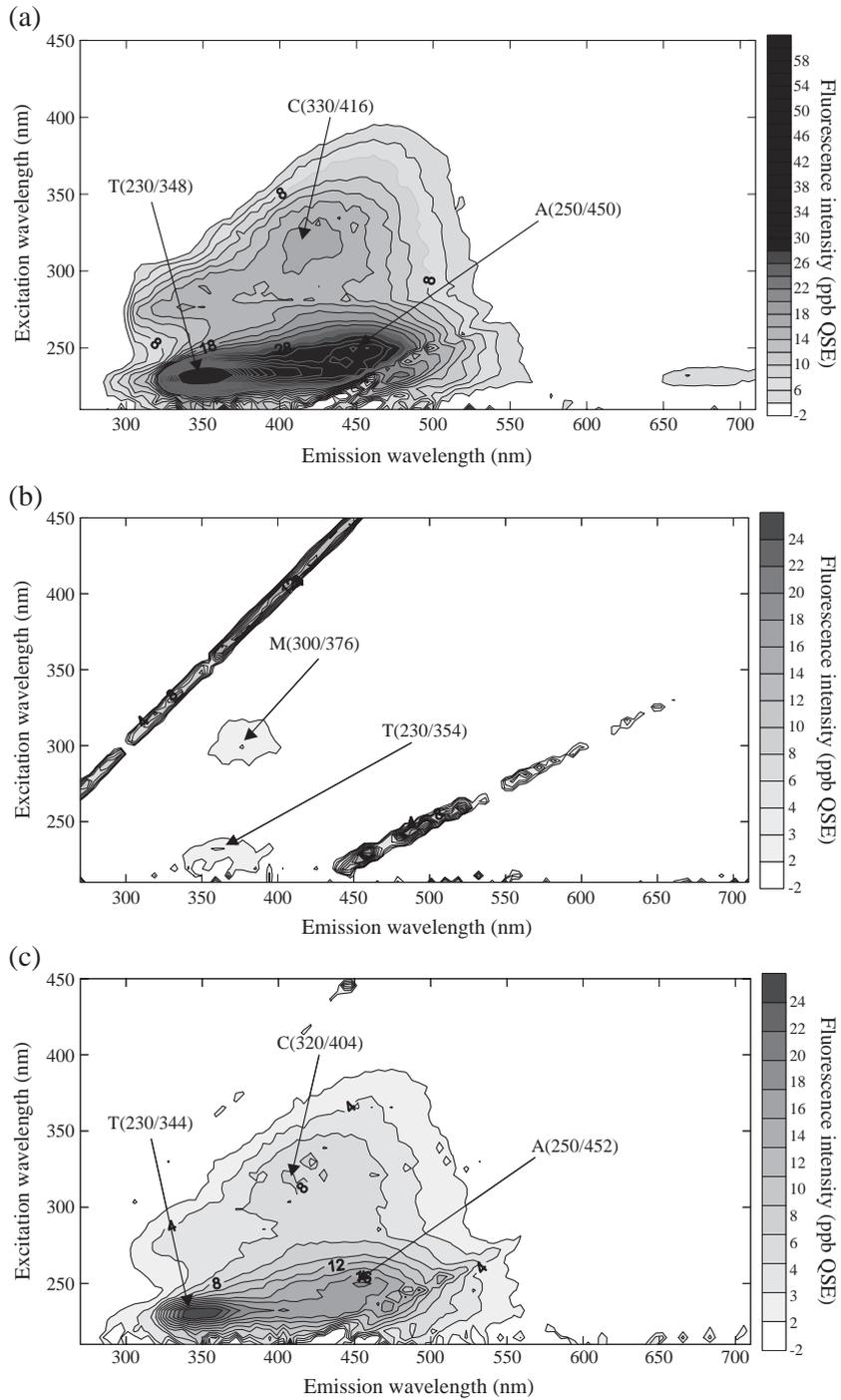
Fig. 6. Contour plots of fluorescence matrices for (a) Station 28 at 1 m; (b) Station 7 at 5 m; (c) Station 20 at 1 m. The position of the excitation–emission maxima is shown in the plots.

and 325/416 for T, A and C, respectively). T/A/C ratios (reported as T/A/C with $C = 1$) were obtained from water samples collected in the vicinity of Hengmen (Station 14, 3.3/2.1), Hongqimen (Station 18, 1.9/1.5), Jiaomen (Station 30, 3.7/2.5), and Humen outlets (Station 28, 4.3/2.5). The lowest T-proportion (1.9) was found at Station 18, which was mainly influenced by Hongqimen outflow. The highest T-proportion (4.3) occurred near Humen outlet. These are consistent with the model results of Pang and Li (2001) wherein the flux of pollutants at the four main outlets was highest for the Humen outlet and lowest for the Hongqimen outlet. This result shows that terrestrial CDOM input is multi-source in this region. These sources should have had similar $a(355)$ values and similar fluorophores, but instead had different T/A/C ratios. This result also shows the potential for using T/A/C ratios as indices for pollutant identification. However, as data collected in the dry season were limited, this result is not statistically conclusive. Note that because the fluorescence data had not been corrected for instrumental optical aberrations (Coble et al., 1993), the fluorescence intensity is presented here only in a relative sense. It cannot be compared with data measured with other instruments.

4. Summary and conclusion

Through extensive sampling in the Pearl River Estuary, a complex environment that receives substantial terrestrial inputs from various sources, we measured the absorption and fluorescence characteristics of chromophoric dissolved organic matter (CDOM) in the low flow (dry) season. Our objective was to investigate the abundance, sources, and nature of CDOM in the Pearl River Estuary for a season during which no CDOM data had been previously reported.

Using standard absorption and fluorescence analysis techniques, we found that for a 33–0 salinity range CDOM absorption coefficients at 355 nm, $a(355)$, ranged from 0.24 to 1.93 m^{-1}. In comparison with other major river systems, these CDOM values were relatively low. In contrast to results from wet seasons, $a(355)$ results obtained in November (2002) showed a linear, inverse relationship with salinity,

suggesting a freshwater source and conservative mixing. Relatively high $a(355)$ values in the vicinity of Hengmen, Hongqimen, Jiaomen and Humen outlets, suggested multiple terrestrial CDOM sources. Discharge from each outlet plays a role in controlling the spatial distribution patterns of CDOM in the estuary.

CDOM compositional analysis produced two principal results. (1) In the transition zone between the estuary and South China Sea shelf water, samples appeared to have lower absorption spectral slopes (S) than those observed in riverine water. A marine humic-like fluorophore (M) was observed in the transition zone by EX/EM spectroscopic analysis. This phenomenon can be interpreted as a mixing process involving upstream estuarine water and adjacent seawater with different S values. The seawater included not only open South China Sea shelf water but also Yuedong Coastal Current and heavily polluted Hong Kong coastal water. Photobleaching and bacterial utilization in combination with changes in CDOM sources might play a role as well. (2) Fluorophore T was the strongest of three distinct fluorophores (T, A, and C) for all samples, and had fluorescence features similar to those from animal farm wastes. T/A/C intensity ratios varied in the vicinity of different outlets. The proportion of T (relative to C) was highest for the Humen outlet and lowest for the Hongqimen outlet, possibly corresponding to differences in the fluxes of pollutants through these outlets. Hence, it may be possible to distinguish various CDOM sources with EX/EM spectroscopic analysis. However, as the data were collected from only one season and only one sample was collected in the vicinity of each outlet, this work needs to be continued into the wet season and extended to include water end members directly from various outlets.

Comparison of CDOM absorption and chlorophyll-*a* concentration (Chl*a*) from all water samples showed that the estuary corresponded to a typical Case-II water type where Chl*a* neither dominated the optical signal nor co-varied with CDOM. In particular, most optical variations were from CDOM, not from Chl*a*. This presents a great challenge in attempts to distinguish Chl*a* from CDOM via satellite observations. Efforts to develop a regional algorithm based on these results, as well as on other optical measurements (e.g., surface reflectance), are currently underway.

Acknowledgements

References

Baker, A., 2002. Fluorescence properties of some farm wastes: implications for water quality monitoring. Water Res. 36, 189–195.

Battin, T., 1998. Dissolved organic matter and its optical properties in a blackwater tributary of the upper Orinoco River, Venezuela. Org. Geochem. 28, 561–569.

Blough, N.V., Del Vecchio, R., 2002. Chromophoric DOM in the coastal environment. In: Hansell, D., Carlson, C. (Eds.), Biogeochemistry of Marine Dissolved Organic Matter. Academic Press, San Diego, CA, pp. 509–546.

Blough, N.V., Zafiriou, O.C., Bonilla, J., 1993. Optical absorption spectra of waters from the Orinoco River outflow: terrestrial input of colored organic matter to the Caribbean. J. Geophys. Res. 98, 2271–2278.

Callahan, J., Dai, M., Chen, R.F., Li, X.L., Lu, Z.M., Huang, W., 2004. Dissolved organic matter in the Pearl River Estuary, China. Mar. Chem. 89, 211–224.

Carder, K.L., Steward, R.G., Harvey, G.R., Ortner, P.B., 1989. Marine humic and fulvic acids: their effects on remote sensing of ocean chlorophyll. Limnol. Oceanogr. 34, 68–81.

Chen, X., Li, Z., Zeng, F., Yun, Z., Xu, Z., 1993. Hydrological and water quality characteristics of the tidal river networks on the Pearl River Delta. Proceedings of International Workshop on the Development of Strategies for Pollution Control in the Pearl River Delta, pp. 101–109.

Chen, C.Q., Shi, P., Yin, K.D., Pan, Z., Zhan, H.G., Hu, C.M., 2003. Absorption coefficient of yellow substance in the Pearl River Estuary. SPIE 4892, 215–221.

Chen, Z.Q., Li, Y., Pan, J.M., 2004. The distributions of the optical properties of colored dissolved organic matter and dissolved organic carbon in the Pearl River Estuary. Cont. Shelf Res. 24, 1845–1856.

Coble, P.G., 1996. Characterization of marine and terrestrial DOM in seawater using excitation emission matrix spectroscopy. Mar. Chem. 51, 325–346.

Coble, P.G., Mopper, K., Schultz, C.S., 1993. Fluorescence contouring analysis of DOC intercalibration experiment samples: a comparison of techniques. Mar. Chem. 41, 173–178.

Coble, P.G., Del Castillo, C.E., Avril, B., 1998. Distribution and optical properties of CDOM in the Arabian Sea during the 1995 Southwest Monsoon. Deep-Sea Res. II 45, 2195–2223.

Del Castillo, C.E., Coble, P.G., Morell, J.M., Lopez, J.M., Corredor, J.E., 1999. Analysis of the optical properties of the Orinoco river plume by absorption and fluorescence spectroscopy. Mar. Chem. 66, 35–51.

Del Castillo, C.E., Coble, P.G., Conmy, R.N., Muller-Karger, F.E., Vanderbloomen, L., Vargo, G.A., 2001. Multispectral in-situ measurements of organic matter and chlorophyll fluorescence in seawater: documenting the intrusion of the Mississippi River Plume in the West Florida Shelf. Limnol. Oceanogr. 46 (7), 1836–1843.

Ferrari, G.M., 2000. The relationship between chromophoric dissolved organic matter and dissolved organic carbon in the European Atlantic coastal area and in the West Mediterranean Sea (Gulf of Lions). Mar. Chem. 70, 339–357.

Ferrari, G.M., Dowell, M.D., 1998. CDOM absorption characteristics with relation to fluorescence and salinity in coastal areas of the southern Baltic Sea. Estuar. Coast. Shelf Sci. 47, 91–105.

Fogg, G.E., Boalch, G.T., 1958. Extracellular products in pure cultures of a brown alga. Nature 181, 789–790.

Gao, H., Zepp, R.G., 1998. Factors influencing photoreactions of dissolved organic matter in a coastal river of the southeastern Unite States. Environ. Sci. Technol. 32, 2940–2946.

Green, S.A., Blough, N.V., 1994. Optical absorption and fluorescence properties of chromophoric dissolved organic matter in natural waters. Limnol. Oceanogr. 39, 1903–1916.

Hu, C., Muller-Karger, F.E., Zepp, R.G., 2002. Absorbance, absorption coefficient, and apparent quantum yield: a comment on common ambiguity in the use of these optical concepts. Limnol. Oceanogr. 47, 1261–1267.

Hu, C., Muller-Karger, F.E., Biggs, D.C., Carder, K.L., Nababan, B., Nadeau, D., Vanderbloomen, J., 2003. Comparison of ship and satellite bio-optical measurements on the continental margin of the NE Gulf of Mexico. Int. J. Remote Sens. 24, 2597–2612.

Huang, X.P., Huang, L.M., Yue, W.Z., 2003. The characteristics of nutrients and eutrophication in the Pearl River Estuary, China. Mar. Pollut. Bull. 47, 30–36.

Kirk, J.T.O., 1994. Light and Photosynthesis in Aquatic Ecosystems. Cambridge University Press, Cambridge.

Markager, S., Vincent, W.F., 2000. Spectral light attenuation and absorption of UV and blue light in natural waters. Limnol. Oceanogr. 45 (3), 642–650.

Mitchell, B.G., Bricaud, A., Carder, K., Cleveland, J., Ferrari, G.M., Gould, R., Kahru, M., Kishino, M., Maske, H., Moisan, T., Moore, L., Nelson, N., Phinney, D., Reynolds, R.A., Sosik, H., Stramski, D., Tassan, S., Trees, C., Weidemann, A., Wieland, J.D., Vodacek, A., 2000. Determination of spectral absorption coefficients of particles, dissolved material and phytoplankton for discrete water samples. In: Fargion, G.S., Mueller, J.L., McClain, C.R. (Eds.), Ocean Optics Protocols For Satellite Ocean Color Sensor Validation, Revision 2, NASA Technical Memorandum, vol. 2000-209966, pp. 125–153. Chapter 12.

Momzikoff, A., Dallot, S., Gondry, G., 1994. Distribution of seawater fluorescence and dissolved flavins in the Almeria-Oran

front (alboran Sea, western Mediterranean Sea). J. Mar. Syst. 5, 361–376.

Mopper, K., Schultz, C.A., 1993. Fluorescence as a possible tool for studying the nature and water column distribution of DOC components. Mar. Chem. 41 (1–3), 229–238.

Moran, M.A., Sheldon, W.M., Zepp, R.G., 2000. Carbon loss and optical property changes during long-term photochemical and biological degradation of estuarine dissolved organic matter. Limnol. Oceanogr. 45, 1254–1264.

Morel, A., Prieur, L., 1977. Analysis of variations in ocean color. Limnol. Oceanogr. 22, 709–722.

Nieke, B., Reuter, R., Heuermann, R., Wang, H., Babin, M., Therriault, J.C., 1997. Light absorption and fluorescence properties of chromophoric dissolved organic matter (CDOM) in the St. Lawrence Estuary (Case 2 waters). Cont. Shelf Res. 17, 235–252.

Pang, Y., Li, Y.X., 2001. Effects of discharged pollutions form Pearl River Delta on east outlets. J. Hohai Univ. 29 (4), 50–55 (in Chinese with English abstract).

Pearl River Water Resources Commission, Ministry of Water Resources, China, 2000. Report of water resources of the Pearl River in 1999. Pearl River 6, 1–3, 21.

Qian, H., Liang, S., 1999. Study on the red tide in the Pearl River estuary and its near waters. Mar. Environ. Sci. 18, 69–74 (in Chinese with English abstract).

Rochelle-Newall, E.J., Fisher, T.R., 2002. Chromophoric dissolved organic matter and dissolved organic carbon in Chesapeake Bay. Mar. Chem. 77, 23–41.

Siddorn, J.R., Bowers, D.G., Hoguane, A.M., 2001. Detection the Zambezi River plume using observed optical properties. Mar. Pollut. Bull. 42 (10), 942–950.

Siegel, D.A., Michaels, A.F., 1996. Quantification of non-algal light attenuation in the Sargasso Sea: implications for biogeochemistry and remote sensing. Deep-Sea Res. II 43, 321–345.

Siegel, D.A., Maritorena, S., Nelson, N.B., Hansell, D.A., Lorenzi-Kayser, M., 2002. Global distribution and dynamics of colored dissolved and detrital organic materials. J. Geophys. Res. 107, 3228. doi:10.1029/2001JC000965.

Stedmon, C.A., Markager, S., Kaas, H., 2000. Optical properties and signatures of chromophoric dissolved organic matter (CDOM) in Danish coastal waters. Estuar. Coast. Shelf Sci. 51, 267–278.

Vodacek, A., Blough, N.V., DeGrandpre, M.D., Peltzer, E.T., Nelson, R.K., 1997. Seasonal variation of CDOM and DOC in the Middle Atlantic Bight: terrestrial inputs and photo-oxidation. Limnol. Oceanogr. 42 (4), 674–686.

Yentsch, C.S., Reichert, C.A., 1961. The interrelationship between water-soluble yellow substances and chloroplastic pigments in marine algae. Bot. Mar. 3, 65–74.